Acta Oceanol. Sin., 2017, Vol. 36, No. 5, P. 51–56
DOI: 10.1007/s13131-016-0885-y
http://www.hyxb.org.cn
E-mail: hyxbe@263.net

Dramatic weakening of the ear-shaped thermal front in the Yellow Sea during 1950s–1990s

Tana[1, 2], FANG Yue[2, 3]*, LIU Baochao[2], SUN Shuangwen[2, 3], WANG Huiwu[2]

[1] College of Oceanic and Atmospheric Sciences, Ocean University of China, Qingdao 266100, China

[2] Center for Ocean and Climate Research, The First Institute of Oceanography, State Oceanic Administration, Qingdao 266061, China

[3] Laboratory for Regional Oceanography and Numerical Modeling, Qingdao National Laboratory for Marine Science and Technology, Qingdao 266235, China

Received 16 February 2016; accepted 14 March 2016

Abstract

The ear-shaped thermal front (ESTF), formed by the convergence of the Yellow Sea Warm Current (YSWC) and the Shandong Coastal Current (SCC), is a very important oceanic phenomenon in the Yellow Sea (YS) in winter. *In situ* measurements and reanalysis datasets all demonstrate that the ESTF has been weakening during 1950s–1990s, and a similar weakening trend is also found in winter monsoon over the YS. Numerical experiments show that the weakening of winter monsoon can induce an anomalous circulation in the YS on multi-decadal timescale with northward anomalous currents along China's coast and southward anomalous currents in the central YS—generally opposite to seasonal mean circulation. The anomalous circulation causes slowdown of the YSWC and the SCC, and thus weakens the ESTF. Since the ESTF plays important roles in regional ocean dynamics and air-sea interactions, its weakening has important implications for regional climate in the YS in winter.

Key words: thermal front, Yellow Sea, circulation, monsoon, multi-decadal variability

Citation: Tana , Fang Yue, Liu Baochao, Sun Shuangwen, Wang Huiwu. 2017. Dramatic weakening of the ear-shaped thermal front in the Yellow Sea during 1950s–1990s. Acta Oceanologica Sinica, 36(5): 51–56, doi: 10.1007/s13131-016-0885-y

1 Introduction

Observations and numerical models both show that there exists many thermal fronts, with complicated spatial distributions, in the Yellow Sea in winter. Among those thermal fronts, the one located to the east coast of the Shandong Peninsular, which is called ear-shaped thermal front (ESTF) (also called N-shaped thermal front) according to the geometry of its horizontal distribution, is most remarkable in terms of spatial scale and intensity (Zheng and Klemas, 1982; He et al., 1995; Wang and Liu, 2009; Huang et al., 2010). Like the other thermal fronts in the Yellow Sea, the ESTF shows obvious seasonal and interannual variabilities on its location, intensity, and distribution (Wang and Liu, 2009). The variation of the ESTF has important implications for oceanic processes (including sediment transport and deposition), marine ecosystem and fishery, and local or regional synoptic and climatic systems (sea fog, precipitation, etc.).

The East Asian monsoon system has experienced significant variations during the past few decades due to the global climate change. Calculation based on the monthly winds from NCEP/NCAR reanalysis (Kalnay et al., 1996) shows that the mean wind speed of January from 1951 to 1970 over the Yellow Sea, which is 5.9 m/s, decreases by more than 15% to a mean of 5.0 m/s in 1981–2000. Since the monsoon is the dominant influencing factor on physical characteristics of the Yellow Sea in winter, in particular the circulation pattern and the temperature distribution, the ESTF is expected to vary accordingly on multi-decadal timescale as monsoon changes. However, previous studies on the variations of the ESTF are mainly focused on its seasonal or interannual variability. In present study, *in situ* observations, reanalysis datasets, and satellite measurements will be used to investigate the multi-decadal variation of the ESTF, including its characteristics and mechanism.

2 Multi-decadal variation of the ESTF

Figure 1a shows the climatological mean of sea surface temperature (SST) in February from the AVHRR Pathfinder Version 5.2 (PFV5.2) data (Casey et al., 2010). The SST on the eastern and western sides of the Yellow Sea is obvious colder than that in the central basin. In the eastern coastal region to the Shandong Peninsula, isotherms of 6–8°C are closely distributed basically along the 50 m isobath and form a very strong thermal front. To objectively locate the position of the front, a mathematical model based on gravity algorithm (Ping et al., 2013) is applied to the SST in Fig. 1a and all the detected thermal fronts are shown in Fig. 1b. One can see that there is, as discovered by many existing studies (e.g., Zheng and Klemas, 1982; Hickox et al., 2000; Huang et al., 2010), a very strong front in (35.5°–38.0°N, 122.0°–123.5°E), roughly parallel to the coastline of the Shandong Peninsula with an ear-like

Foundation item: The National Basic Research Program (973 Program) of China under contract No. 2012CB955601; the National Natural Science Foundation of China under contract Nos 41576028 and 41306032; the NSFC Shandong Joint Fund for Marine Science Research Centers under contract No. U1606405; the Basic Scientific Research Fund for National Public Institutes of China under contract Nos GY2010T02 and GY2014G27.

*Corresponding author, E-mail: yfang@fio.org.cn

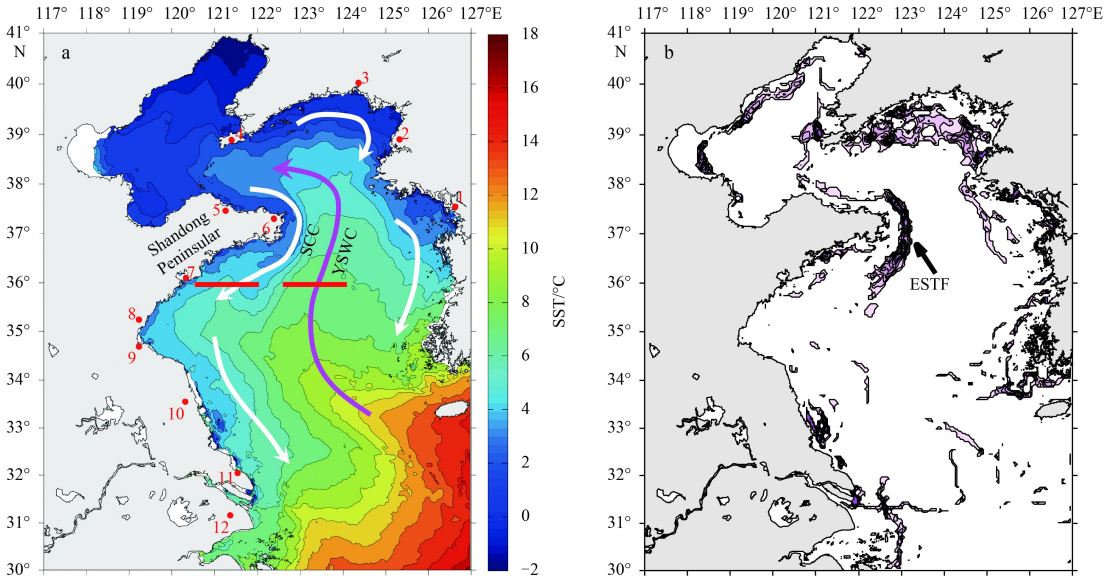

Fig. 1. Schematic pattern of the Yellow Sea circulation in winter and locations of 12 coastal weather stations (a), and thermal fronts detected by a mathematical model based on gravity algorithm (b). 1. Seoul, 2. Pyongyang, 3. Dandong, 4. Dalian, 5. Yantai, 6. Chengshantou, 7. Qingdao, 8. Rizhao, 9. Ganyu, 10. Sheyang, 11. Nantong, and 12. Xujiahui.

shape.

In the Yellow Sea, observational data covering a long time period are very rare. In the region where the ESTF is located, the only available *in situ* temperature observations in winter covering a relative long time period were collected along the section of 36°N, 120.5°–124.5°E in February of each year start from 1977. Previous studies [see the review by Ichikawa and Beardsley (2002)] have suggested that the Yellow Sea in winter can be considered as a barotropic ocean because it is shallow (mean water depth is less than 45 m) and the vertical mixing induced by surface cooling and monsoonal winds is strong—this characteristic is also exhibited by the observed temperature along 36°N (Fig. 2a). Therefore, the SST distribution well represents the horizontal temperature distribution of the entire water column below the surface, and thus the SST gradient cross a thermal front can reasonably reflect the intensity of the front. Since the 36°N section just crosses the southern part of the ESTF, the SST gradient at 122°15′E, where the maximum temperature gradient is located (Fig. 2a), can be used as an index of the ESTF intensity. To make calculation simple, we deduct the mean temperature of 120.5°–122 °E (west section) from that of 122.5°–124°E (east section) and use the calculated difference as an alternative of the temperature gradient at 122°15′E. It worth to be noted that the SST in the Yellow Sea has been rising during the past few decades due to the global warming effects, but the rising in SST is basin—wide and can be approximately treated as uniform warming along the west and east sections considering that the spatial size of the two sections are small and their locations are very close to each other. With the above method, the effects of global warming on SST can be effectively canceled and the ESTF intensity can be well estimated and its variation is plotted in Fig. 2b. The ESTF we noted, in addition to its interannual variability, has been weakening persistently since the beginning of the observation and lasts till around 1995.

To further valid the multi-decadal trend in variation of the ESTF intensity, same calculations are applied to the daytime SST of PFV5.2 and the temperature at 2.5 m from the China Ocean Reanalysis (CORA) (Han et al., 2011) and the results are also shown in Fig. 2b. The CORA is based on the Princeton Ocean Model with generalized coordinate system (POMgcs) and assimilates various sources of observations including satellite remote sensing SST, altimetry sea level anomaly, and *in situ* temperature and salinity profiles. Evaluations of the CORA demonstrate that this reanalysis dataset provides a good representation, with high resolution, of the seasonal and interannual variabilities of the SST in coastal waters of China and adjacent seas (Wu et al., 2013). Although the variations of the ESTF intensity illustrated by the three different datasets in Fig. 2b show some differences in interannual signals, the persistent weakening trend before the 1990s in these three time series are quite similar, and the weakening is quite dramatic—the temperature difference drops markedly from approximately 3.5–2°C.

3 Mechanism of the ESTF weakening

The surface winds are mainly northerly over the Yellow Sea in winter, and coastal currents are basically southward due to the forcing of the surface winds. Since the Yellow Sea is a semiclosed marginal sea, there must be a current going to the north in the central Yellow Sea to compensate the mass lost caused by the southward coastal currents. The compensating current is the well-known Yellow Sea Warm Current (YSWC), which transports warm water from lower to higher latitudes and has been extensively studied during the past few decades (Kondo, 1985; Guan, 1986, Fang et al., 1997; Lin and Yang, 2011). Previous studies have demonstrated that the ESTF, just like many other thermal fronts in the Yellow Sea in winter, is a product of convergence of cold coastal current and the YSWC (Ma et al., 2006; Wang and Liu, 2009). In the case of ESTF formation, the cold costal current is the Shandong Costal Current (SCC). The location, shape, and intensity of the ESTF vary significantly on seasonal and interannual timescales, and the variation is closely linked to the variability of winter monsoon (Wang and Liu, 2009).

Is the weakening of the ESTF shown in Fig. 2c related to the variation of the circulation in the Yellow Sea and the winter monsoon? Since there is no long-term *in situ* observation for the currents in the Yellow Sea, we have to turn to the SODA dataset (Car-

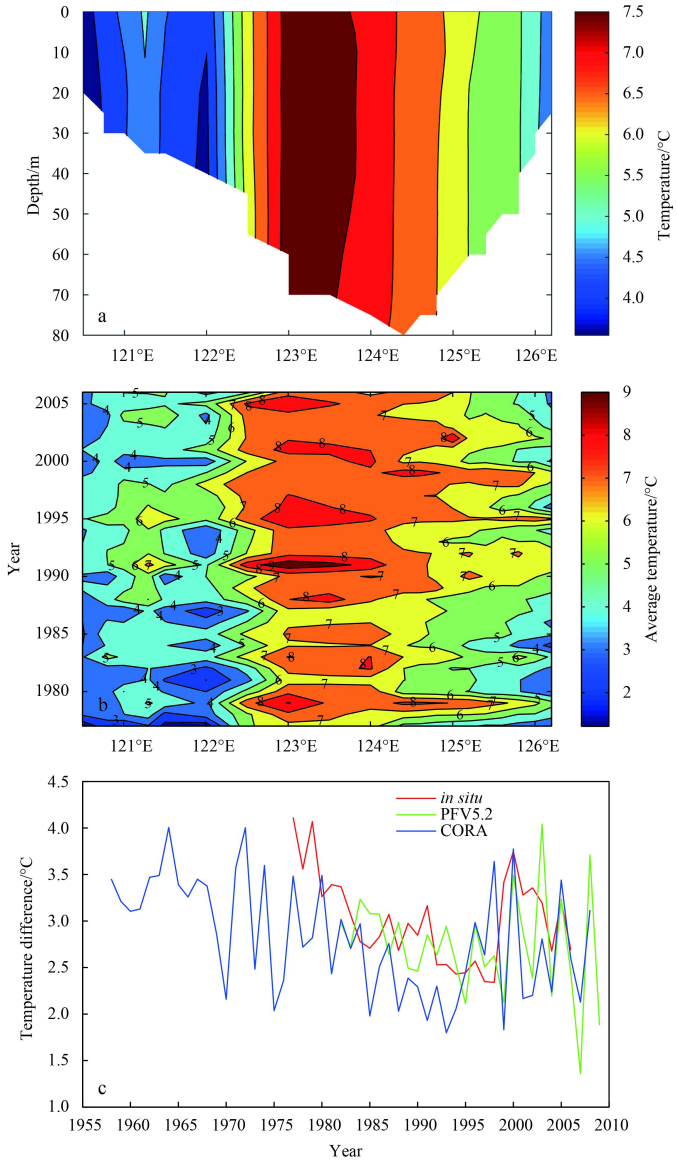

Fig. 2. Temperature distribution along 36°N in February averaged from *in situ* observations in 1977–2006 (a), variation of the temperature averaged from 0 m to 20 m in February along 36°N (b) and surface temperature difference in February between sections of 120.5°–122.0°E and 122.5°–124.0°E (the latter minus the former; refer to the red lines in Fig. 1a) along 36°N (c). Red line: *in situ* observations, green line: AVHRR PFV5.2, and blue line: China Ocean Reanalysis (CORA).

ton and Giese, 2008) that has been widely used in studying ocean circulation and climate, though its reconstructed circulations in marginal seas are not as reliable as those in open oceans. To investigate the change in currents on multi-decadal time scale in the region where the ESTF is located, we first define the time period of 1956–1975 as "positive phase" when the ESTF is relatively intense, and that of 1976–1995 as "negative phase" when the ESTF is relatively weak. The way of partitioning these two phases is justified, because 1976–1977 is usually considered as an important point in time of the so-called "climate shift" (or "regime shift") in the climate system over the North Pacific Ocean (Trenberth and Hurrell, 1994; Miller et al., 1994). The Yellow Sea in winter, as mentioned above, is approximately a barotropic ocean, so the distribution of the currents averaged vertically can well represent the general circulation pattern. Figure 3a shows the difference of January currents between the positive and negative phases (the later minus the former) derived from the SODA dataset. It is clear that the major change in circulation is characterized by anomalous northward currents along China's coastal waters and anomalous southward currents in the central Yellow Sea. These anomalous currents are generally opposite to the mean circulation of this season, suggesting that both the YSWC and the coastal currents are weaker in the negative phase. Under such circumstance, the temperature contrast between the water masses advected by the SCC and the YSWC to the east of the Shandong Peninsula is reduced, and weaker ESTF is thus expected.

On the basis of mechanisms of the formation of the YSWC and coastal currents in winter, we conjecture that the weakening of the circulation in the Yellow Sea on multi-decadal timescale, similar to the variation on interannual timescale, is also resulted from monsoon variability. To test this hypothesis, we derive the change in January surface winds between the positive and negative phases from the NCEP/NCAR reanalysis dataset, and, for

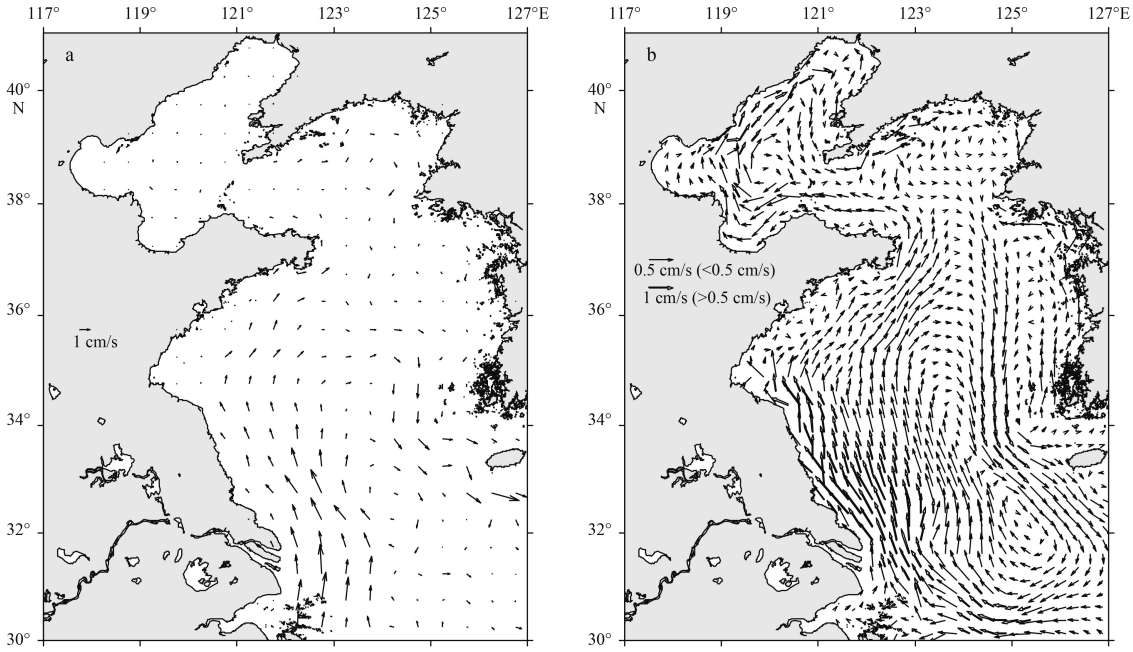

Fig. 3. Difference in January circulation (vertically averaged) between the positive phase (1958–1975) and the negative phase (1976–1995) (the later minus the former) derived from the SODA dataset (a) and simulations from a 2-D barotropic ocean model forced with surface winds from NCEP/NCAR reanalysis (b).

comparison, similar calculation is also applied to the surface winds from the ERA-40 reanalysis dataset (Uppala et al., 2005) (Fig. 4a). The anomalous wind fields derived from the two different datasets overall agree to each other very well, albeit differences do exist in magnitude and direction. The anomalous winds over the Yellow Sea are dominating southerlies, indicating weaker monsoons in the negative phase. The variation of the wind speed averaged over the entire Yellow Sea basin in January further reveals the weakening trend of monsoon during 1950s–1990s (Fig. 4b), well in phase with that of the ESTF shown in Fig. 2c.

To further verify the multi-decadal variability of the winter monsoon over the Yellow Sea, historical wind speed observed in January at 12 coastal weather stations are plotted in Fig. 4c. Although these stations are land-based and the winds they measured are usually weaker than those in open waters, they are all adjacent to the Yellow Sea and thus the variation of the observed wind speed should be in phase with those over the Yellow Sea. One can see that the wind speeds at all the weather stations exhibit an obvious decreasing trend before the 1990s, which disappears after the 1990s—a feature identical to the one shown in Fig. 4b, suggesting that the weakening of winter monsoon over the Yellow Sea in the 1950s–1990s is robust.

Is the weakening of winter monsoon over the Yellow Sea a major cause for the anomalous circulation shown in Fig. 3a? Considering that the Yellow Sea during wintertime is a barotropic shallow sea, a two-dimensional numerical model should be able to reproduce the general circulation in the season. Here we adopt the two-dimensional ocean model established by Fang et al. (1996), which has been widely used to study the wintertime circulations in China's adjacent seas (e.g., Fang et al., 1997, 2000, 2001). Configuration of the model, such as computation domain, boundary conditions, parameters, etc., also follows Fang et al. (1997). To explore the influence of winter monsoon on the circulation of the Yellow Sea during 1950s–1990s, two numerical experiments are conducted, in which climatological January wind fields of the positive and negative phases from the NCEP/NCAR reanalysis are used respectively as the only surface forcing in the model. After the numerical integration of each experiment reaches a stable state, the simulated current field can thus be treated as the climatological circulation of the Yellow Sea corresponding to each (warm/cold) phase. Figure 3b shows the difference in circulation simulated by the two experiments. It can be seen that the change in circulation, no matter the YSWC or the coastal currents, agrees very well with that derived from the SODA (Fig. 3a). Since the only difference between the two experiments is the surface wind, we can conclude that the anomalous circulations shown in Fig. 3 are mainly induced by the weakening of winter monsoon during 1950s–1990s.

There are another two mechanisms that may also play a role in the formation of the ESTF. One is the one-dimensional bathymetric-control mechanism proposed by Xie et al. (2002), in which the thermal inertia of water column in the Yellow Sea is argued to be linearly proportional to the bottom depth and responsible for the strong association between the SST and bottom topography distributions. The other one is the tide-induced upwelling mechanism (Lü et al., 2010), in which a secondary circulation is triggered by baroclinic gradient across the tidal mixing fronts, bringing cold bottom water to surface to form a thermal front. The effects of this mechanism is most visible in summertime SST distributions [see Figs 3 and 9b of Lü et al. (2002)]. However, the multi-decadal variability of the key factors (bathymetry and tide, respectively) of those two mechanisms are negligible, so the two mechanisms have little connection with the dramatic weakening of the ESTF.

4 Summary and discussion

The ESTF, formed by the convergence of the YSWC and the SCC, is a very important oceanic phenomenon in the Yellow Sea in winter. *In situ* measurements, satellite data, and reanalysis datasets all demonstrate that the ESTF has been weakening dur-

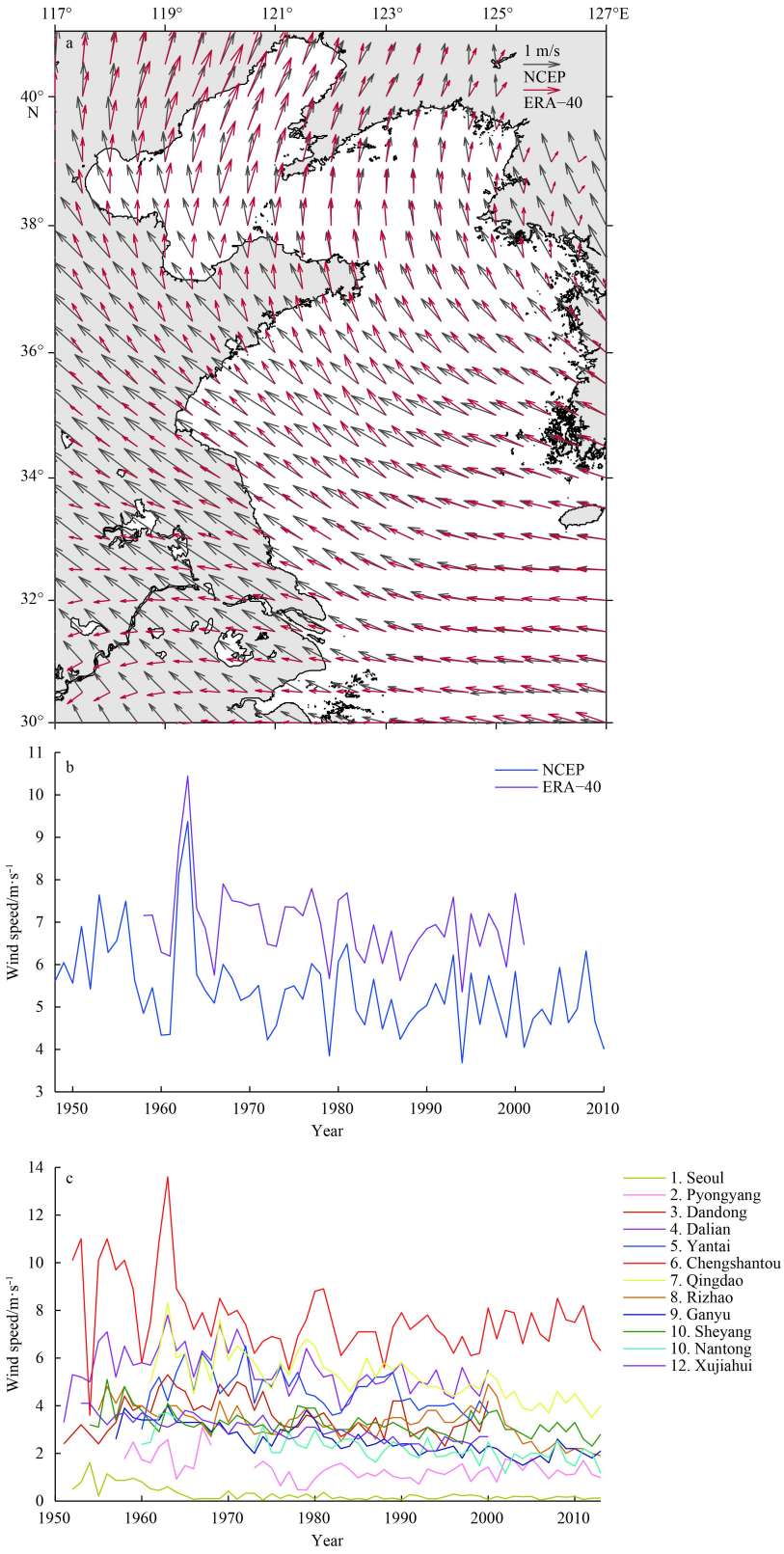

Fig. 4. Multi-decadal variability of the surface winds in January over the Yellow Sea and adjacent regions. Difference in January surface wind fields between the positive phase (1958–1975) and the negative phase (1976–1995) (the later minus the former) derived from the NCEP/NCAR (black arrows) and ERA-40 (red arrow) datasets (a), interannual variations of January surface wind speed averaged over the entire Yellow Sea basin based on the NCEP (blue line) and ERA-40 (purple line) datasets (b), and interannual variations of January wind speed observed at 12 coastal weather stations surrounding the Yellow Sea (see Fig. 1a for locations of the weather stations) (c).

ing 1950s–1990s. Similar weakening trend is also found in winter monsoon over the Yellow Sea from reanalysis datasets, and this trend is further confirmed by historical observations at land-based weather stations surrounding the Yellow Sea. The numerical experiments of a barotropic ocean model show that the weakening of winter monsoon can induce an anomalous circulation with a northward anomalous flow along China's coast and a southward anomalous flow in the central basin of the Yellow Sea, which is in general opposite to seasonal mean circulation. The anomalous circulation causes slow down of the YSWC and the SCC, and thus weakens the ESTF. Considering the roles that the ESTF plays in ocean dynamics and air-sea interactions, the weakening of the ESTF has important implications for regional climate in the Yellow Sea in winter.

Although in the present study the dynamical influence of the multi-decadal variability of the East Asian winter monsoon on the circulation of the Yellow Sea well explains the dramatic weakening of the ESTF during 1950s–1990s, physical processes related to heat fluxes that are involved in the variability of the ESTF have not been quantitively examined due to the limitation of the simple barotropic ocean model adopted. It is worth to note that the monsoonal wind speed of January over the Yellow Sea decreases by approximately 15% (this number is even smaller if based on the ERA-40 reanalysis) during the 1950s–1990s, while the simulated volume transport of the YSWC is reduced by about 20%–25% (varies with latitudes) and the reduction in the ESTF intensity can be more than 30%. This suggests that the intensity of the ESTF is very sensitive to the strength of monsoon, thus a numerical model with more complete dynamics is necessary in the future for studying the ESTF variability.

Acknowledgements

NCEP reanalysis dataset is provided by the NOAA/OAR/ESRL PSD (http://www.esrl.noaa.gov/psd/); ERA-40 reanalysis dataset is prepared by the European Centre for Medium-range Weather Forecasts (http://apps.ecmwf.int/datasets/); *in situ* SST data are provided by the National Marine Data and Information Service, State Oceanic Administration, China; SODA reanalysis can be downloaded from http://soda.tamu.edu/data.htm; CORA reanalysis dataset is provided by the WMO-IOC Centre for Marine Meteorological and Oceanographic Climate Data (http://www.cmoc-china.cn/web/guest/access-to-metadata). AVHRR Pathfinder Version 5.2 (PFV5.2) data are obtained from the US National Oceanographic Data Center and GHRSST (http://pathfinder.nodc.noaa.gov).

References

Carton J A, Giese B S. 2008. A reanalysis of ocean climate using Simple Ocean Data Assimilation (SODA). Mon Wea Rev, 136(8): 2999–3017

Casey K S, Brandon T B, Cornillon P, et al. 2010. The past, present, and future of the AVHRR Pathfinder SST Program. In: Barale V, Gower J F R, Alberotanza L, eds. Oceanography from Space. Dordrecht: Springer, 273–287.

Fang Yue, Fang Guohong, Wang Kai, et al. 2001. Dynamics of the Kuroshio intrusion into the southeast China adjacent waters—A numerical study. J Hydrodynamics: Ser B, 13(3): 28–33

Fang Yue, Fang Guohong, Yu Kejun. 1996. ADI barotropic ocean model for simulation of Kuroshio intrusion into China southeastern waters. Chin J Oceanol Limnol, 14(4): 357–366

Fang Yue, Fang Guohong, Zhang Qinghua. 2000. Numerical simulation and dynamic study of the wintertime circulation of the Bohai Sea. Chin J Oceanol Limnol, 18(1): 1–9

Fang Yue, Zhang Qinghua, Fang Guohong. 1997. A numerical study on the path and origin of the Yellow Sea Warm Current. The Yellow Sea, 3: 18–26

Guan Bingxian. 1986. Current structure and its variation in equatorial area of the western North Pacific Ocean. Chin J Oceanol Limnol, 4(3): 239–255

Han Guijun, Li Wei, Zhang Xuefeng, et al. 2011. A regional ocean reanalysis system for coastal waters of China and adjacent seas. Adv Atmos Sci, 28(3): 682–690

He Mingxia, Ge Chen, Sugimori Y. 1995. Investigation of mesoscale fronts, eddies and upwelling in the China seas with satellite data. Global Atmos Ocean Syst, 3(4): 273–288

Hickox R, Belkin I, Cornillon P, et al. 2000. Climatology and seasonal variability of ocean fronts in the East China, Yellow and Bohai Seas from satellite SST data. Geophys Res Lett, 27(18): 2945–2948

Huang Daji, Zhang Tao, Zhou Feng. 2010. Sea-surface temperature fronts in the Yellow and East China Seas from TRMM microwave imager data. Deep-Sea Res: Part II, 57(11–12): 1017–1024

Ichikawa H, Beardsley R C. 2002. The current system in the Yellow and East China Seas. J Oceanogr, 58(1): 77–92

Kalnay E, Kanamitsu M, Kistler R, et al. 1996. The NCEP/NCAR 40-year reanalysis project. Bull Amer Meteor Soc, 77(3): 437–470

Kondo M. 1985. Oceanographic investigations of fishing ground in the East China Sea and the Yellow Sea: I. Characteristics of the mean temperature and salinity distributions measured at 50 m and near the bottom. Bull Seikai Reg Fish Lab, 62: 19–66

Lin Xiaopei, Yang Jiayan. 2011. An asymmetric upwind flow, Yellow Sea Warm Current: 2. Arrested topographic waves in response to the northwesterly wind. J Geophys Res, 116(C4): C04027, doi: 10.1029/2010JC006514

Lü Xingang, Qiao Fangli, Xia Changshui, et al. 2010. Upwelling and surface cold patches in the Yellow Sea in summer: effects of tidal mixing on the vertical circulation. Continental Shelf Research, 30(6): 620–632

Ma Jian, Qiao Fangli, Xia Changshui, et al. 2006. Effects of the Yellow Sea Warm Current on the winter temperature distribution in a numerical model. J Geophys Res, 111(C11): C11S04, doi: 10.1029/2005JC003171

Miller A J, Cayan D R, Barnett T P, et al. 1994. The 1976–77 climate shift of the Pacific Ocean. Oceanography, 7(1): 21–26

Ping Bo, Su Fenzhen, Du Yunyan, et al. 2013. Application of the model of universal gravity to oceanic front detection near the Kuroshio front. J Geo-Inf Sci (in Chinese), 15(2): 187–192

Trenberth K E, Hurrell J W. 1994. Decadal atmosphere-ocean variations in the Pacific. Climate Dyn, 9(6): 303–309

Uppala S M, Kallberg P W, Simmons A J, et al. 2005. The ERA-40 reanalysis. Q J R Meteorol Soc, 131(131): 2961–3012

Wang Fan, Liu Chuanyu. 2009. An N-shape thermal front in the western South Yellow Sea in winter. Chin J Oceanol Limnol, 27(4): 898

Wu Yang, Cheng Guosheng, Han Guijun, et al. 2013. Analysis of seasonal and interannual variability of sea surface temperature for China seas based on CORA dataset. Haiyang Xuebao (in Chinese), 35(1): 44–54

Xie Shangping, Hafner J, Tanimoto Y, et al. 2002. Bathymetric effect on the winter sea surface temperature and climate of the Yellow and East China Seas. Geophys Res Lett, 29(24): 81–1–81–4, doi: 10.1029/2002GL015884

Zheng Quanan, Klemas V. 1982. Determination of winter temperature patterns, fronts, and surface currents in the Yellow Sea and East China Sea from satellite imagery. Remote Sensing of Environment, 12(3): 201–218